Graefe's Archive for Clinical and Experimental Ophthalmology
https://doi.org/10.1007/s00417-026-07265-6

RESEARCH

Multimodal evaluation of choroidal vascular alterations after panretinal photocoagulation in diabetic retinopathy

Areum Jeong[1] · Ye Eun Han[2] · Leegoni Choi[2] · Dahye Jung[2] · Yulim Kim[2] · Min Sagong[1] · Junyeop Lee[2,3]

Received: 31 October 2025 / Revised: 11 March 2026 / Accepted: 21 April 2026

Abstract

Purpose To evaluate morphological and quantitative changes in the choroid after panretinal photocoagulation (PRP) for diabetic retinopathy using multimodal imaging and to identify factors associated with these changes.

Methods This retrospective study included 48 eyes of 26 patients with severe non-proliferative or proliferative diabetic retinopathy. Ultra-widefield indocyanine green angiography (UWF-ICGA) and enhanced-depth imaging optical coherence tomography (EDI-OCT) were performed before and after PRP. Choroidal vessel density, fractal dimension (FD), and hyperpermeable area were quantified from fluorescein angiography-subtracted ICGA images using ImageJ and Fractalyse software. Choroidal vascularity index (CVI), subfoveal choroidal thickness (SFCT), and Haller's layer thickness were measured on EDI-OCT. CVI was calculated as the ratio of the luminal area to the total subfoveal choroidal area within a 1,500-μm region. Relationships among choroidal and retinal parameters were analyzed by multivariable regression.

Results After PRP, the mean hyperpermeable area significantly decreased (8.78%→7.95%, $p<0.001$), accompanied by reductions in choroidal vessel density (34.67%→33.34%, $p<0.001$), FD (1.662→1.632, $p=0.003$), SFCT (266.63→242.75 μm, $p<0.001$), and CVI (64.34%→62.13%, $p<0.001$). Haller's layer thickness was independently associated with the hyperpermeable area, while CVI correlated with central retinal thickness and Haller's layer thickness.

Conclusion PRP reduces choroidal vascular congestion and complexity, suggesting structural remodeling of the choroidal vasculature associated with reduced vascular permeability. Quantitative ICGA- and OCT-derived indices may serve as noninvasive biomarkers for evaluating choroidal remodeling and treatment response after PRP in diabetic retinopathy.

Key Messages

What is known

- Panretinal photocoagulation (PRP) is the standard treatment for proliferative diabetic retinopathy, but its impact on the choroidal vasculature remains incompletely understood, with previous studies reporting inconsistent findings regarding post-PRP choroidal thickness and perfusion changes.

What is new

- Quantitative multimodal imaging revealed significant reductions in choroidal hyperpermeability, vascular density, fractal dimension, and choroidal vascularity index after PRP, indicating decreased vascular congestion and complexity.
- Haller's layer thickness was independently associated with the hyperpermeable area, suggesting that large choroidal vessels are particularly responsive to PRP-associated changes in choroidal vascular permeability.
- These findings support the concept that PRP is associated with reductions in choroidal vascular congestion and complexity, suggesting structural remodeling of the choroidal vasculature, and that ICGA- and OCT-derived metrics may serve as noninvasive biomarkers of choroidal remodeling and treatment response in diabetic retinopathy.

Keywords Panretinal photocoagulation · Choroidal vascular remodeling · Choroidal vascular density · Fractal dimension · Choroidal vascularity index · Choroidal thickness · Ultra-widefield ICGA · Enhanced-depth imaging OCT

Areum Jeong and Ye Eun Han contributed equally to this work.

Extended author information available on the last page of the article

Published online: 01 May 2026

Introduction

Diabetic retinopathy (DR) is a leading cause of vision loss among working-age adults worldwide [1]. Although DR has traditionally been considered a microvascular disease of the retina, increasing evidence suggests that the choroid also undergoes substantial structural and functional alterations in diabetes [2–4]. The choroidal vasculature plays a critical role in maintaining outer retinal homeostasis by supplying oxygen and nutrients to the retinal pigment epithelium and photoreceptors [5]. Therefore, disruption of choroidal perfusion may exacerbate retinal ischemia and contribute to disease progression [6].

Advances in enhanced-depth imaging optical coherence tomography (EDI-OCT) and ultra-widefield indocyanine green angiography (UWF ICGA) have enabled detailed visualization of choroidal morphology and circulation [4, 7, 8]. These imaging modalities have revealed various features of diabetic choroidopathy, including choriocapillaris dropout, vessel dilation, and areas of hyperpermeability [9–11]. However, the relationship between these choroidal changes and the clinical course or treatment response of DR remains incompletely understood.

Panretinal photocoagulation (PRP) is the standard therapy for proliferative diabetic retinopathy (PDR), aiming to reduce ischemic drive and vascular endothelial growth factor (VEGF) expression [12]. Despite its proven efficacy in preventing severe vision loss, PRP may induce secondary effects on the choroidal circulation. Previous reports have shown inconsistent findings—some demonstrating transient thickening and others persistent thinning of the choroid after PRP—likely due to differences in imaging protocols and timing of evaluation [13–17]. Quantitative metrics such as the choroidal vascularity index (CVI) and fractal dimension (FD) can provide objective measures of vascular remodeling and complexity, yet few studies have integrated these parameters with UWF ICGA-based assessments of choroidal hyperpermeability and vascular density [18–20].

Recently, we reported that qualitative and quantitative analyses of UWF ICGA images revealed progressive dilation, complexity, and hyperpermeability of choroidal vessels with advancing stages of DR [4]. Building upon these findings, the present study aimed to evaluate the morphological and quantitative changes in the choroidal vasculature before and after PRP in eyes with severe non-proliferative diabetic retinopathy (NPDR) and PDR. Using multimodal imaging including UWF ICGA and EDI-OCT, we analyzed choroidal vascular density, area of hyperpermeability, FD, and CVI. This study provides comprehensive insight into how PRP influences choroidal vascular structure and function, thereby improving understanding of diabetic choroidopathy as both a disease manifestation and a modifiable treatment target.

Methods

Patients

This study was a retrospective observational case series. This study was approved by the Internal Review Board of the Yeungnam university medical center. Informed consent was obtained from all patients, and the study adhered to the tenets of the Declaration of Helsinki. This study included patients with DR who underwent four sessions of PRP at intervals of two weeks to one month and had available UWF ICGA obtained within one month before the initiation of PRP and within two months after the completion of PRP. Patients were excluded if either of the two ICGA image was unsuitable for analysis due to media opacity or other image quality issues. Forty-eight eyes (26 patients) with a diagnosis of severe NPDR or PDR were included in this study. Exclusion criteria included high myopia or hyperopia (greater than −6 or +3 diopters of refractive error), poor image quality, history of anti-VEGFs or laser photocoagulation, any other associated retinal pathology, history of any intraocular surgery, or ocular diseases that could potentially cause retinal or choroidal vascular changes (e.g., any type of macular degeneration, including age-related macular degeneration, central serous chorioretinopathy, retinal vascular occlusion, or intraocular inflammation). All participants underwent a comprehensive ophthalmic examination including best-corrected visual acuity testing, slit-lamp biomicroscopy, intraocular pressure measurement, and dilated fundoscopic examination. All patients underwent OCT, ultra-wide-field fluorescein angiography (UWF FA) and UWF ICGA before and after four sessions of PRP.

UWF angiographic parameters

After pupil dilation, UWF FA and UWF ICGA images were acquired using a UWF retinal imaging device (Optos California ultra-widefield imaging device; Dunfermline, Scotland, UK). Simultaneous UWF FA and ICGA were performed after an intravenous injection of 5 mL of 10% sodium fluorescein and 25 mg of ICG. Images were obtained during the early phase, mid and late phases of the angiogram. Choroidal vascular abnormalities were defined as ICGA findings not evident with FA.

Both qualitative and quantitative assessments of choroidal vascular features were conducted.To exclude fluorescent signals derived from the optic disc and retinal vessels from the ICGA images, the FA images were subtracted from the

ICGA images using ImageJ software (National Institutes of Health, Bethesda, Maryland, USA; available at http://rsb.info.nih.gov/ij/index.html). Binarized images of the choroidal vessels were obtained, as previously reported[47]. Choroidal vascular hyperpermeability was evaluated in late phase ICGA. For other measurement, all images were transformed to a stereographic projection image using prototype software from the manufacturer. Hyperpermeable area was defined as the area was brighter than vortex vein fluorescence. We manually demarcated the outline of the hyperpermeable area and calculated in pixels using ImageJ. The area of hyperpermeability was calculated using the following formula: (area of hyperpermeability)/(total area) X 100 (%). The total area and the area with choroidal vessels were calculated in pixels using the ImageJ. The choroidal vessel density was calculated using the following formula: (area with choroidal vessels)/(total area) X 100 (%). The FD is a measure of vasculature branching pattern complexity[48]. We used Fractalyse software version 2.4 (http://www.fractalyse.org/). Fractalyse software enables measuring FD by box-counting method. The FD varies with the distribution of vessels in the image and has a value between 0 and 2. The more complex the vessel, the higher the measured value.

OCT-based choroidal parameters

EDI-OCT scans of the macula were performed using Spectralis OCT (Heidelberg Engineering, Heidelberg, Germany). EDI-OCT was used to visualize the choroidal vascular layers: the choriocapillaris layer, the choroidal layer composed of medium-sized vessels (Sattler's layer), and the large-vessel choroidal layer (Haller's layer). Horizontal 6-mm line scans through the center of fovea were obtained. Only scans with sufficient image quality were used for quantitative analysis.

Central retinal and subfoveal choroidal thickness (SFCT) were measured at foveal center using in-built calipers tool provided in the software (Heidelberg Eye Explorer, version 1.10.1.0; Heidelberg Engineering). CVI was defined as the proportion of luminal area to the total circumscribed subfoveal choroidal area measured on fovea-centered EDI-SD-OCT images. CVI was calculated based on the protocol previously described [42, 47] with modifications using ImageJ software (version 1.52, Wayne Rasband, National Institutes of Health; Bethesda, MD, USA). Concisely, the subfoveal choroidal area with a width of 1,500 µm (750 µm on each side of fovea), was selected and added to the region of interest (ROI) manager (see Supplementary Fig. S3 online). After image binarization, the dark pixels were selected using colour threshold tool and added to the ROI manager. The total subfoveal circumscribed area, area of dark pixels (luminal area), and area of light pixels (stromal area) were calculated. CVI was calculated by dividing luminal area by total circumscribed subfoveal choroidal area. Two masked graders (A.J. and Y.E.H.) independently performed SFCT and CVI measurements. Interobserver reproducibility was assessed using intraclass correlation coefficients: SFCT = 0.936 (95% confidence interval [CI] = 0.892–0.960, $p < 0.001$), CVI = 0.947 (95% CI = 0.936–0.953, $p < 0.001$).

Table 1 Demographic and clinical characteristics

	N=26 Patients, 48 Eyes
Age (years)	60.6±11.1 (36–81)
Gender (Male/Female)	25 (52.1%) / 23 (47.9%)
Laterality (Right/ Left)	26 (54.2%) / 22 (45.8%)
DR stage (severe NPDR/PDR)	30 (62.5%) / 18 (37.5%)
BCVA (LogMAR)	0.23±0.20
Spherical Equivalent (Diopters)	-0.48±2.21
Central retinal thickness (µm)	287.73±58.01

Statistical analysis

Statistical analysis was performed using SPSS version 21.0 (IBM Corp., Armonk, NY, USA). The values were analyzed using the paired-t test for comparing before and after laser treatment. Univariate and multivariable linear regression analyses were performed to determine the associations of area of choroidal hyperpermeability with ocular factors. For multivariate linear regression, factors showing suggestively significant association in univariate analysis ($P<0.10$) were included. All P values were considered statistically significant when the values were <0.05.

Results

Baseline characteristics of eyes

A total of 48 eyes from 26 subjects were included in this study. The mean age was 60.6±11.1 years,25 male (52.1%) and 23 female (47.9%) subjects. The distribution of eyes was 26 (54.2%) in the right eye, 22 (45.8%) in the left eye. Thirty eyes (62.5%) had severe NPDR, and 18 eyes (37.5%) had PDR. The mean best corrected visual acuity was 0.23±0.20 LogMAR, and the mean spherical equivalent was −0.48±2.21 diopters. The mean central retinal thickness was 287.73±58.01 micrometers (Table 1).

Qualitative changes in UWF ICGA following PRP

Four major qualitative angiographic features of ICGA were summarized in Supplementary Fig. S1 and S2. (1) Hypofluorescent spots: a delay in dye filling or choriocapillaris defects in early phase ICGA. (2) Salt and pepper pattern:

Table 2 Qualitative and quantitative ICGA features before and after PRP

	Baseline	After PRP	*P*-value
Early ICGA Hypofluorescent spots	31 (64.6%)	36 (75.0%)	0.069
ICGA salt and pepper pattern	25 (52.1%)	31 (64.6%)	0.182
Early inverted flow phenomenon	5 (10.4%)	8 (16.7%)	0.675
Late choroidal non-perfusion region	30 (62.5%)	40 (83.3%)	<0.001
Area of choroidal hyperpermeability (%)	8.78±4.68	7.95±6.98	<0.001
Choroidal vascular density (%)	34.67±0.94	33.34±1.16	<0.001
Fractal dimension	1.662±0.041	1.632±0.435	0.003

lobular spotty hyperfluorescent and hypofluorescent mottled pattern in the posterior pole in the very late phase ICGA. (3) Early inverted flow phenomenon: choroidal vessel filling time was longer than retinal vessel filling time. (4) Choroidal non-perfusion region: choroidal non-perfusion area in late phase ICGA. Among 48 eyes, 31 eyes (64.6%) had hypofluorescent spots before PRP, 36 eyes (75.0%) had it after PRP. Twenty five eyes (52.1%) had the patchy pattern, described as a salt and pepper pattern before PRP, 31 eyes (64.6%) had it after PRP. Early inverted flow phenomenon was observed in 5 eyes (10.4%) before PRP, 8 eyes (16.7%) after PRP. Choroidal non-perfusion region was seen in 30 eyes (62.5%) before PRP, 40 eyes (83.3%) after PRP. Choroidal non-perfusion region was only significantly different between before and after PRP ($p<0.001$) (Table 2) .

Quantitative changes in UWF ICGA following PRP

The overall image processing workflow used for quantitative assessment of choroidal vasculature is summarized in Fig. 1, illustrating each step from raw angiographic imaging to fractal analysis. The mean area of hyperpermeability was 8.78±4.68% before PRP, 7.95±6.98% after PRP. Mean area of hyperpermeability was significantly decreased after PRP ($p<0.001$) (Table 2). Multivariable linear regression demonstrated that area of choroidal hyperpermeability was significantly correlated with Haller's layer ($p=0.001$) (Table 3). Before PRP, mean choroidal vascular density was 34.67±0.94% and it was 33.34±1.16% after PRP. The mean choroidal vascular dentisy before PRP were significantly higher than that after PRP ($p<0.001$) (Table 2). Before PRP, eyes had a higher mean FD (1.662±0.041 vs. 1.632±0.435), the difference was significant ($p= 0.003$) (Table 2). A representative case of UWF ICGA and quantitative choroidal vascular analysis before and after PRP is shown in Fig. 2.

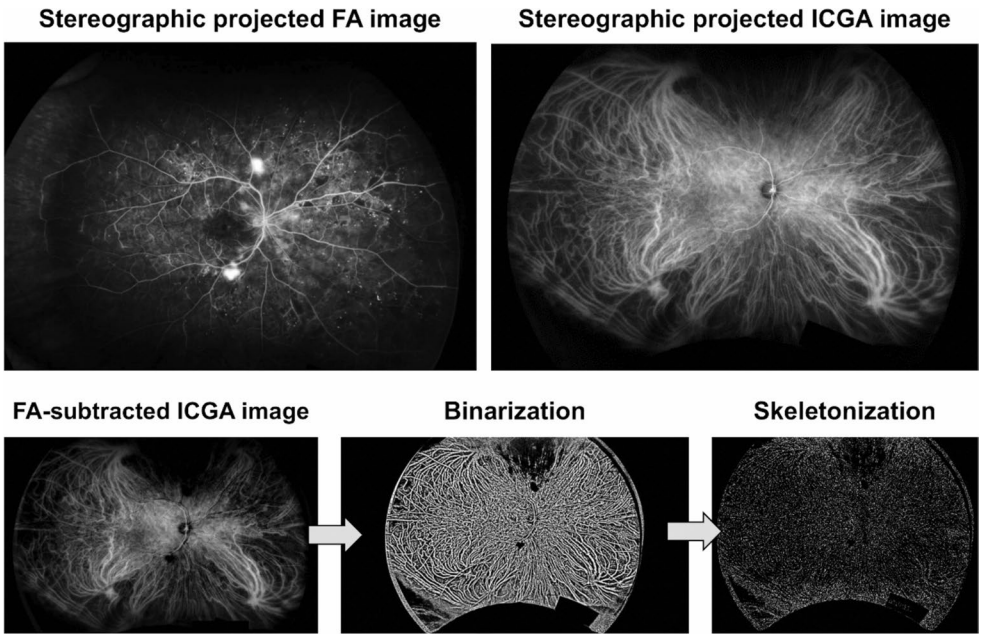

Fig. 1 Image processing workflow for choroidal vascular analysis. Stereographic projected fluorescein angiography (FA) and indocyanine green angiography (ICGA) images were obtained using an ultra-widefield imaging system. The FA images were subtracted from the ICGA images using ImageJ software (National Institutes of Health, Bethesda, MD, USA) to generate FA-subtracted ICGA images highlighting the choroidal vasculature. Binarization and skeletonization were applied to extract vascular networks for quantitative analysis. Choroidal vessel density was calculated after binarization as (vascular area / total area) × 100, and fractal dimension , representing vascular branching complexity, was measured after binarization and skelectonization using Fractalyse software version 2.4

Table 3 Linear regression analyses of factors associated with area of choroidal hyperpermeability

Variables	Univariate		Multivariable	
	β	*P*-value	β	*P*-value
Age (years)	0.276	0.073		
Diabetic macular edema	0.222	0.153		
Hypertension	-0.292	0.101		
DR stage	-0.137	0.380		
BCVA (LogMAR)	-0.113	0.469		
Central retinal thickness (μm)	-0.252	0.103		
Subfoveal choroidal thickness (μm)				
Sattler's layer	0.052	0.741		
Haller's layer	-0.523	0.001*	-0.482	0.001*
Choroidal vascularity index (%)	-1.178	0.246	-0.159	0.262
Fractal dimension	-0.179	0.250	-0.133	0.351

Quantitative changes in OCT parameters following PRP

The mean SFCT were 266.63 ± 37.25 μm before PRP, 242.75 ± 34.32 μm after PRP. SFCT was decreased significantly after PRP ($p < 0.001$). Similar trends were observed for Sattler's layer (from 55.35 ± 9.62 μm to 51.58 ± 11.02 μm; $P < 0.001$) and Haller's layer (from 211.27 ± 36.90 μm to 191.17 ± 36.11 μm; $P < 0.001$). There was a statistically significant decrease in CVI after PRP (62.13 ± 1.82) compared to the baseline (64.34 ± 1.42; $p < 0.001$) (Table 4). A representative OCT changes in choroidal parameters before and after PRP is shown in Fig. 3. Multivariable linear regression demonstrated that area of CVI was significantly correlated with effective central retinal thickness and thickness of Haller's layer ($P = 0.003$, $P = 0.001$, respectively) (Table 5).

Table 4 Choroidal thickness and choroidal vascularity index before and after PRP

	Baseline	After PRP	*P*-value
Subfoveal choroidal thickness (μm)	266.63 ± 37.25	242.75 ± 34.32	< 0.001
Sattler's layer	55.35 ± 9.62	51.58 ± 11.02	< 0.001
Haller's layer	211.27 ± 36.90	191.17 ± 36.11	< 0.001
Choroidal vascularity Index (%)	64.34 ± 1.42	62.13 ± 1.82	< 0.001

Discussion

Normal choroidal vascular structure and circulation are essential for maintaining retinal function [21]. Therefore, understanding the choroidal structure and blood flow is critical to elucidating disease pathophysiology. Previous studies have shown that laser photocoagulation can destruct the choriocapillaris, as demonstrated by scanning laser ophthalmoscopy with ICGA or by choroidal microsphere counts [22].

In this study, we investigated ICGA patterns in eyes with severe NPDR and PDR to identify possible vascular changes at the level of the choroidal circulation after PRP. PRP significantly reduced choroidal vascular density, complexity, and

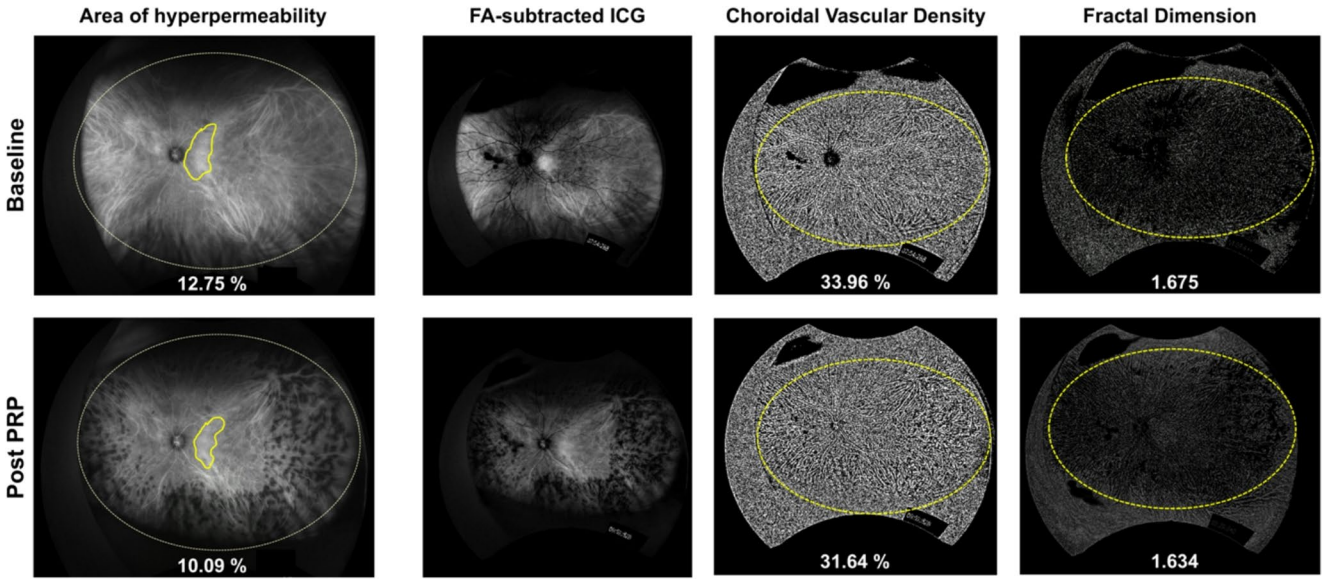

Fig. 2 Representative ultra-widefield ICGA and quantitative choroidal vascular analysis before and after PRP. Ultra-widefield ICGA images demonstrate a reduction in the area of choroidal hyperpermeability after panretinal photocoagulation (PRP) in a 56-year-old patient with proliferative diabetic retinopathy (PDR). FA-subtracted ICGA, binarized, and skeletonized images were processed as shown in Fig. 1 to quantify choroidal vascular parameters within the analyzed region (yellow outline). Following PRP, the area of choroidal hyperpermeability decreased from 12.75% to 10.09%, accompanied by reductions in choroidal vascular density (33.96% to 31.64%) and fractal dimension (1.675 to 1.634), indicating reduced vascular congestion and complexity in the choroidal vasculature

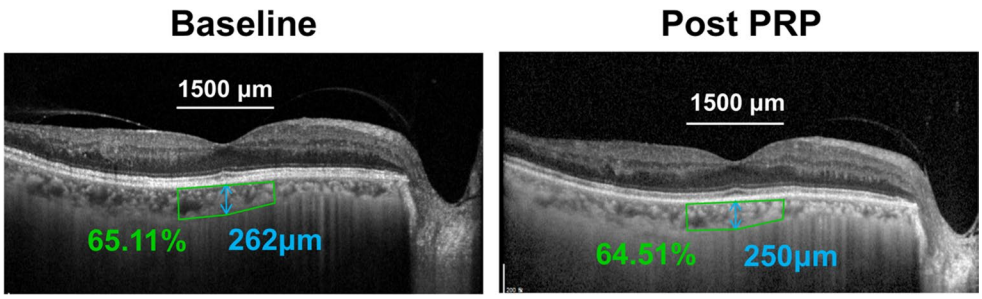

Fig. 3 Representative OCT changes in choroidal parameters before and after PRP. Optical coherence tomography (OCT) B-scans from a 54-year-old patient with proliferative diabetic retinopathy demonstrate decreased subfoveal choroidal thickness (SFCT) and choroidal vascular index (CVI) following panretinal photocoagulation (PRP). The SFCT was reduced from 262 µm to 250 µm, and the CVI decreased from 65.11% to 64.51%. These findings indicate a post-PRP reduction in choroidal vascular congestion and luminal area, suggesting indicating reduced vascular congestion and complexity in the choroidal vasculature

Table 5 Linear regression analyses of factors associated choroidal vascularity index

Variables	Univariate		Multivariable	
	β	*P*-value	β	*P*-value
Age (years)	-0.068	0.244		
Gender	-0.035	0.627		
Diabetic macular edema	0.127	0.104		
Hypertension	-0.094	0.258		
DR stage	-0.062	0.795		
BCVA (LogMAR)	-0.164	0.131		
Area of choroidal hyperpermeability (%)	-0.158	0.224		
Central retinal thickness (µm)	-0.142	0.036	-0.059	0.003
Subfoveal choroidal thickness (µm)				
Sattler's layer	0.362	<0.001	0.0.546	0.381
Haller's layer	0.488	<0.001	0.375	0.001
Fractal dimension	-0.012	0.354	-0.144	0.151

thickness. Our recent investigation on diabetic choroidopathy demonstrated that both choroidal vascular density and FD progressively increased with advancing stages of diabetic retinopathy, reflecting compensatory or maladaptive vascular remodeling [4]. The present study extends these observations by showing that such large choroidal vascular changes in diabetes appear to shift toward a less congested vascular pattern following PRP. This suggests that the reduction in retinal ischemic drive after PRP may influence angiogenic signaling and choroidal vascular dynamics, to which large choroidal vessels respond most sensitively, resulting in partial restoration of vascular architecture and function [23].

In addition, we observed a significant increase in late-phase choroidal non-perfusion areas after PRP. However, other qualitative biomarkers including hypofluorescent spots, salt-and-pepper appearance, and inverted inflow phenomenon, showed not significant change. Nevertheless, these parameters exhibited subtle aggravation of these inflammatory signs immediately after PRP. This finding implies that PRP, while therapeutically effective, may transiently exacerbate choroidal inflammation due to acute laser-induced metabolic and vascular stress [24]. Therefore, short-term post-PRP evaluations should be interpreted with caution, and further longitudinal follow-up is warranted to clarify whether these transient inflammatory responses eventually stabilize or evolve into chronic choroidal alterations over time.

The mechanism by which oxygen supply is increased after PRP is multifactorial [25]. First, the retina in the laser-treated region becomes thinner, bringing the choriocapillaris and inner retina into closer proximity. Second, destruction of photoreceptors—cells with high oxygen demand—reduces the metabolic consumption of the outer retina within laser scars [26–28]. Because PRP disrupts portions of the retinal pigment epithelium (RPE) and outer retina, it may secondarily influence the choroidal circulation [29]. Evaluating changes in choroidal perfusion therefore provides valuable insight into the pathophysiology and progression of DR. However, only a few studies have examined choroidal alterations before and after PRP in diabetic eyes.

Histopathological studies have demonstrated choriocapillaris dropout in diabetes, which progresses with worsening DR [30]. Upregulation of vascular endothelial growth factor (VEGF) in response to RPE and photoreceptor hypoxia can lead to vasodilation of medium and large choroidal vessels [31]. Moreover, decreases in the choroidal luminal area have been reported after anti-VEGF therapy in diabetic macular edema and polypoidal choroidal vasculopathy [32, 33].

Our findings revealed that PRP in eyes with severe NPDR and PDR significantly reduced choroidal vascular density, FD, SFCT, and CVI. Several studies have also reported a post-PRP reduction in choroidal thickness, total choroidal area, luminal area, and choroidal blood flow compared with untreated eyes [29, 34–36]. Aiello et al. [37] demonstrated that vitreous VEGF concentrations in PDR are higher than in NPDR and significantly decrease after successful PRP. In chronic hyperglycemic states, choroidal vessels often

exhibit excessive dilation, tortuosity, and hyperpermeability—hallmarks of endothelial dysfunction [19, 38]. PRP may alter angiogenic and inflammatory signaling pathways, potentially influencing choroidal vascular behavior between angiogenic and anti-angiogenic signaling, resulting in a more stable and less permeable vascular network.

Alterations in choroidal circulation may directly influence oxygen and nutrient delivery to the outer retina. Reduced hyperpermeability and vascular congestion after PRP could facilitate more efficient oxygen diffusion and metabolic exchange at the RPE–photoreceptor interface [15, 39]. Conversely, excessive reduction in choroidal perfusion might lead to secondary ischemia in the outer retina, underscoring the importance of maintaining an optimal PRP energy balance that preserves choroidal support while suppressing neovascular drive [40, 41].

Quantitative indices such as the CVI and FD, together with UWF ICGA–derived hyperpermeability maps, may serve as noninvasive biomarkers for evaluating choroidal vascular health and treatment response [42–44]. These imaging biomarkers could complement conventional retinal findings in assessing PRP or anti-VEGF efficacy and may help identify eyes at risk of ischemic progression despite adequate laser treatment. In ICGA analyses, the area of hyperpermeability was smaller after PRP. Multivariable regression revealed that Haller's layer thickness was independently associated with the hyperpermeable area, suggesting that PRP may reduce angiogenic drive and thereby decreases choroidal vascular permeability. Reduced vascular leakage and stromal swelling consequently result in choroidal thinning.

Some reports have described a transient increase in choroidal thickness within one week after PRP [24, 45]. Cho et al. [45] speculated that this transient increase may result from vasodilation or choroidal effusion secondary to peripheral choriocapillaris damage, leading to reduced peripheral flow and compensatory redistribution toward the macula. According to Nonaka et al. [24] inflammatory leukocyte–endothelial interactions occur immediately after laser photocoagulation, upregulating nitric oxide synthesis and inducing vasodilation. Because PRP targets the peripheral retina, restriction of peripheral blood flow and redistribution toward the posterior pole may cause a temporary increase in macular perfusion.

Nevertheless, reports on post-PRP choroidal thickness changes remain inconsistent. Such discrepancies may arise from variations in laser protocols, timing of post-treatment measurements, or blood-flow assessment techniques. Furthermore, PRP-induced choroidal changes are likely influenced by multiple inflammatory mediators and cytokines, adding to the complexity of this condition [42, 46]. Future studies combining multimodal imaging with molecular biomarkers may clarify how systemic and local vascular factors contribute to diabetic choroidopathy. Longitudinal investigations could also determine whether PRP-induced choroidal remodeling predicts functional outcomes or suboptimal response to subsequent anti-VEGF therapy. Integrating these structural and molecular metrics into clinical decision-making could advance individualized management of DR.

Previous studies [42, 47] have shown that DR involves central RPE and choroidal structural alterations that may be partially reversible with anti-VEGF therapy. As our OCT analysis was limited to the central 1,500 μm region, the reductions in choroidal thickness and CVI should be interpreted as surrogate markers of central choroidal modulation rather than global remodeling. When considered alongside UWF ICGA findings of reduced choroidal hyperpermeability and vascular complexity, these OCT-derived metrics may still reflect a broader choroidal response to PRP.

This study has several limitations. First, the sample size was relatively small and the follow-up period short. Second, there was no control group. Third, only the central 1,500 μm scan was analyzed as a representative region, which may not fully reflect global choroidal changes. A volume scan covering the macula would provide more detailed spatial information. Fourth, manual image delineation may have introduced observer bias. Fifth, detailed information on systemic diabetic treatment was unavailable, and antidiabetic medications might have influenced choroidal parameters. Finally, structural changes observed on imaging should be interpreted cautiously, as histopathologic confirmation was not obtained.

In conclusion, qualitative ICGA features of diabetic choroidopathy suggesting ischemia and inflammation did not markedly change or showed slight increases after PRP. However, PRP significantly reduced choroidal vascular density, complexity, and thickness—findings that may reflect changes in choroidal vascular permeability and remodeling. Further longitudinal studies are needed to elucidate whether increased choroidal non-perfusion and transient post-laser inflammatory responses ultimately stabilize or contribute to the long-term progression of diabetic chorioretinopathy after PRP.

Supplementary Information The online version contains supplementary material available at https://doi.org/10.1007/s00417-026-07265-6.

Author contributions Conception and design: Areum Jeong, Ye Eun Han, Junyeop Lee: Analysis and interpretation: Areum Jeong, Leegoni Choi, Dahye Jung, Yulim Kim, Junyeop Lee: Data collection: Areum Jeong, Ye Eun Han: Writing – original draft: Areum Jeong, Ye Eun Han: Writing – review & editing: Min Sagong, Junyeop Lee: Overall responsibility: Areum Jeong, Ye Eun Han, Junyeop Lee:

Funding This research was supported by a grant of the Korea Health Technology R&D Project through the Korea Health Industry Development Institute (KHIDI), funded by the Ministry of Health & Welfare, Republic of Korea (grant number: RS-2024-00438689), and the Asan Institute for Life Sciences, Asan Medical Center, Seoul, Korea (2023IP0079-3).

Data availability The datasets used and/or analyzed during this study can be made available by the corresponding author upon reasonable request.

Declarations

Ethics approval This study protocol was reviewed and approved by the Institutional Review Board of Yeungnam University Hospital (approval no. 2020-01-017) and was conducted in accordance with the Declaration of Helsinki. Informed consent for angiographic examination was obtained from all patients. The approval included a waiver of informed consent for the chart review. The study does not include any animal experiments conducted by any of the authors.

Competing interests The authors declare no competing interests.

References

1. Ruta LM, Magliano DJ, Lemesurier R, Taylor HR, Zimmet PZ, Shaw JE (2013) Prevalence of diabetic retinopathy in Type 2 diabetes in developing and developed countries. Diabet Med 30(4):387–398
2. Shiragami C, Shiraga F, Matsuo T, Tsuchida Y, Ohtsuki H (2002) Risk factors for diabetic choroidopathy in patients with diabetic retinopathy. Graefes Arch Clin Exp Ophthalmol 240(6):436–442
3. Wang JC, Lains I, Providencia J, Armstrong GW, Santos AR, Gil P et al (2017) Diabetic Choroidopathy: Choroidal Vascular Density and Volume in Diabetic Retinopathy With Swept-Source Optical Coherence Tomography. Am J Ophthalmol 184:75–83
4. Choi SU, Kim YJ, Lee JY, Lee J, Yoon YH (2023) Qualitative and quantitative evaluation of diabetic choroidopathy using ultra-widefield indocyanine green angiography. Sci Rep 13(1):2577
5. Stefansson E (2006) Ocular oxygenation and the treatment of diabetic retinopathy. Surv Ophthalmol 51(4):364–380
6. Esmaeelpour M, Povazay B, Hermann B, Hofer B, Kajic V, Hale SL et al (2011) Mapping choroidal and retinal thickness variation in type 2 diabetes using three-dimensional 1060-nm optical coherence tomography. Invest Ophthalmol Vis Sci 52(8):5311–5316
7. Vujosevic S, Martini F, Cavarzeran F, Pilotto E, Midena E (2012) Macular and peripapillary choroidal thickness in diabetic patients. Retina 32(9):1781–1790
8. Endo H, Kase S, Saito M, Yokoi M, Takahashi M, Ishida S et al (2020) Choroidal Thickness in Diabetic Patients Without Diabetic Retinopathy: A Meta-analysis. Am J Ophthalmol 218:68–77
9. Kim JT, Lee DH, Joe SG, Kim JG, Yoon YH (2013) Changes in choroidal thickness in relation to the severity of retinopathy and macular edema in type 2 diabetic patients. Invest Ophthalmol Vis Sci 54(5):3378–3384
10. Dou N, Li G, Fang D, Zhang S, Liang X, Yu S (2024) Association between choroidopathy and photoreceptors during the early stage of diabetic retinopathy: a cross-sectional study. Graefes Arch Clin Exp Ophthalmol 262(4):1121–1129
11. Nicolini N, Tombolini B, Barresi C, Pignatelli F, Lattanzio R, Bandello F et al (2022) Assessment of Diabetic Choroidopathy Using Ultra-Widefield Optical Coherence Tomography. Transl Vis Sci Technol 11(3):35
12. Ferris FL 3rd (1991) Photocoagulation for diabetic retinopathy. Early Treatment Diabetic Retinopathy Study Research Group. JAMA 266(9):1263–1265
13. Eleiwa KT, Bayoumy A, Elhusseiny MA, Gamil K, Sharawy A (2020) Longitudinal analysis of subfoveal choroidal thickness after panretinal laser photocoagulation in diabetic retinopathy using swept-source optical coherence tomography. Rom J Ophthalmol 64(3):285–291
14. Kang HM, Lee NE, Choi JH, Koh HJ, Lee SC (2018) Significant Reduction of Both Peripapillary and Subfoveal Choroidal Thickness after Panretinal Photocoagulation in Patients with Type 2 Diabetes. Retina 38(10):1905–1912
15. Okamoto M, Matsuura T, Ogata N (2016) Effects of Panretinal Photocoagulation on Choroidal Thickness and Choroidal Blood Flow in Patients with Severe Nonproliferative Diabetic Retinopathy. Retina 36(4):805–811
16. Park N, Lee IG, Kim JT (2020) Changes in choroidal thickness in advanced diabetic retinopathy treated with pan-retinal photocoagulation using a pattern scanning laser versus a conventional laser. BMC Ophthalmol 20(1):226
17. Zhang Z, Meng X, Wu Z, Zou W, Zhang J, Zhu D et al (2015) Changes in Choroidal Thickness After Panretinal Photocoagulation for Diabetic Retinopathy: A 12-Week Longitudinal Study. Invest Ophthalmol Vis Sci 56(4):2631–2638
18. Hua R, Liu L, Wang X, Chen L (2013) Imaging evidence of diabetic choroidopathy in vivo: angiographic pathoanatomy and choroidal-enhanced depth imaging. PLoS ONE 8(12):e83494
19. Lutty GA (2017) Diabetic choroidopathy. Vis Res 139:161–167
20. Melancia D, Vicente A, Cunha JP, Abegao Pinto L, Ferreira J (2016) Diabetic choroidopathy: a review of the current literature. Graefes Arch Clin Exp Ophthalmol 254(8):1453–1461
21. Nickla DL, Wallman J (2010) The multifunctional choroid. Prog Retin Eye Res 29(2):144–168
22. Lee CJ, Smith JH, Kang-Mieler JJ, Budzynski E, Linsenmeier RA (2011) Decreased circulation in the feline choriocapillaris underlying retinal photocoagulation lesions. Invest Ophthalmol Vis Sci 52(6):3398–3403
23. Lee MY, Park S, Song JY, Ra H, Baek JU, Baek J (2022) Inflammatory cytokines and retinal nonperfusion area in quiescent proliferative diabetic retinopathy. Cytokine 154:155774
24. Nonaka A, Kiryu J, Tsujikawa A, Yamashiro K, Nishijima K, Kamizuru H et al (2002) Inflammatory response after scatter laser photocoagulation in nonphotocoagulated retina. Invest Ophthalmol Vis Sci 43(4):1204–1209
25. Abu El-Asrar AM, Alsarhani WK, AlBloushi AF, Alzubaidi A, Gikandi P, Stefansson E (2025) Effect of panretinal photocoagulation on retinal oxygen metabolism and ocular blood flow in diabetic retinopathy. Acta Ophthalmol 103(4):380–387

26. Stefansson E, Hatchell DL, Fisher BL, Sutherland FS, Machemer R (1986) Panretinal photocoagulation and retinal oxygenation in normal and diabetic cats. Am J Ophthalmol 101(6):657–664
27. Yu DY, Cringle SJ, Su E, Yu PK, Humayun MS, Dorin G (2005) Laser-induced changes in intraretinal oxygen distribution in pigmented rabbits. Invest Ophthalmol Vis Sci 46(3):988–999
28. Gowda A, Wood JPM, Chidlow G, Casson RJ (2025) Laser-induced histopathological changes to the retina: A review. Surv Ophthalmol
29. Iwase T, Kobayashi M, Yamamoto K, Ra E, Terasaki H (2017) Effects of photocoagulation on ocular blood flow in patients with severe non-proliferative diabetic retinopathy. PLoS ONE 12(3):e0174427
30. Cao J, McLeod S, Merges CA, Lutty GA (1998) Choriocapillaris degeneration and related pathologic changes in human diabetic eyes. Arch Ophthalmol 116(5):589–597
31. Kurihara T, Westenskow PD, Gantner ML, Usui Y, Schultz A, Bravo S et al (2016) Hypoxia-induced metabolic stress in retinal pigment epithelial cells is sufficient to induce photoreceptor degeneration. Elife.5.
32. Yokouchi H, Nagasato D, Mitamura Y, Egawa M, Tabuchi H, Misawa S et al (2023) Alterations in choroidal vascular structures due to serum levels of vascular endothelial growth factor in patients with POEMS syndrome. Sci Rep 13(1):10650
33. Nagai N, Suzuki M, Minami S, Kurihara T, Kamoshita M, Sonobe H et al (2019) Dynamic changes in choroidal conditions during anti-vascular endothelial growth factor therapy in polypoidal choroidal vasculopathy. Sci Rep 9(1):11389
34. Mikoshiba Y, Iwase T, Ueno Y, Yamamoto K, Ra E, Terasaki H (2018) A randomized clinical trial evaluating choroidal blood flow and morphology after conventional and pattern scan laser panretinal photocoagulation. Sci Rep 8(1):14128
35. Kim JT, Park N (2020) Changes in choroidal vascular parameters following pan-retinal photocoagulation using swept-source optical coherence tomography. Graefes Arch Clin Exp Ophthalmol 258(1):39–47
36. Li Z, Lu T, Zhou L, Huang C, Zhao H, Liang J et al (2023) Retinal and Choroidal Alterations in Diabetic Retinopathy Treatment using Subthreshold Panretinal Photocoagulation with Endpoint Management Algorithm: A Secondary Analysis of a Randomized Clinical Trial. Ophthalmol Ther 12(4):1867–1880
37. Aiello LP, Avery RL, Arrigg PG, Keyt BA, Jampel HD, Shah ST et al (1994) Vascular endothelial growth factor in ocular fluid of patients with diabetic retinopathy and other retinal disorders. N Engl J Med 331(22):1480–1487
38. Scuderi L, Fragiotta S, Di Pippo M, Abdolrahimzadeh S (2023) The Role of Diabetic Choroidopathy in the Pathogenesis and Progression of Diabetic Retinopathy. Int J Mol Sci.24(12)
39. Rahimi M, Kashani AH, Blair NP, Shahidi M (2022) Alterations in Retinal Vascular and Oxygen Metrics in Treated and Untreated Proliferative Diabetic Retinopathy: A Case Report. Case Rep Ophthalmol 13(3):686–691
40. Karst SG, Beiglboeck H, Scharinger R, Meyer EL, Mitsch C, Scholda C et al (2019) Retinal and Choroidal Perfusion Status in the Area of Laser Scars Assessed With Swept-Source Optical Coherence Tomography Angiography. Invest Ophthalmol Vis Sci 60(14):4865–4871
41. Lin Z, Deng A, Hou N, Gao L, Zhi X (2023) Advances in targeted retinal photocoagulation in the treatment of diabetic retinopathy. Front Endocrinol (Lausanne) 14:1108394
42. Motamed Shariati M, Khazaei S, Yaghoobi M (2024) Choroidal vascularity index in health and systemic diseases: a systematic review. Int J Retina Vitreous 10(1):87
43. Yin C, Zhang S, Guo D, Qin J, Lou H, Zhang G (2025) Diagnostic value of choroidal vascular density in predicting the progression of diabetic retinopathy. Sci Rep 15(1):15671
44. Ra H, Jung Y, Lee SH, Park SW, Chhablani J, Baek J (2024) Quantification of Choroidal Vascular Hyperpermeability on Ultra-Widefield Indocyanine Green Angiography in Macular Neovascularization. Diagnostics (Basel).14(7)
45. Cho GE, Cho HY, Kim YT (2013) Change in subfoveal choroidal thickness after argon laser panretinal photocoagulation. Int J Ophthalmol 6(4):505–509
46. Kinoshita T, Imaizumi H, Shimizu M, Mori J, Hatanaka A, Aoki S et al (2019) Systemic and Ocular Determinants of Choroidal Structures on Optical Coherence Tomography of Eyes with Diabetes and Diabetic Retinopathy. Sci Rep 9(1):16228
47. Han YE, Choi L, Jung D, Kim Y, Kim SJ, Kim YJ, Yoon YH, Lee J (2025) Choroidal Vascular Remodeling and Retinal Response Following Aflibercept Loading in Diabetic Macular Edema. Ophthalmol Sci 0(0):101025

Authors and Affiliations

Areum Jeong[1] · Ye Eun Han[2] · Leegoni Choi[2] · Dahye Jung[2] · Yulim Kim[2] · Min Sagong[1] · Junyeop Lee[2,3]

✉ Junyeop Lee
j.lee@amc.seoul.kr

[1] Department of Ophthalmology, College of Medicine, Yeungnam University, Daegu, South Korea

[2] Department of Ophthalmology, Asan Medical Center, College of Medicine, University of Ulsan, 88, Olympic-ro 43-gil, Songpa-gu, Seoul 05505, South Korea

[3] Graduate School of Health Science and Technology, UNIST, Ulsan, South Korea